Am J Cancer Res 2021;11(6):3252-3262
www.ajcr.us /ISSN:2156-6976/ajcr0122369

Original Article

Genetic variants of *EML1* and *HIST1H4E* in myeloid cell-related pathway genes independently predict cutaneous melanoma-specific survival

Yuanmin He[1,2,3], Hongliang Liu[2,3], Sheng Luo[4], Christopher I Amos[5], Jeffrey E Lee[6], Keming Yang[7], Abrar A Qureshi[8,9], Jiali Han[7,10], Qingyi Wei[2,3,11]

[1]Department of Dermatology, The Affiliated Hospital of Southwest Medical University, Luzhou 646000, Sichuan, China; [2]Duke Cancer Institute, Duke University Medical Center, Durham, NC 27710, USA; [3]Department of Population Health Sciences, Duke University School of Medicine, Durham, NC 27710, USA; [4]Department of Biostatistics and Bioinformatics, Duke University School of Medicine, Durham, NC 27710, USA; [5]Institute for Clinical and Translational Research, Baylor College of Medicine, Houston, TX 77030, USA; [6]Department of Surgical Oncology, the University of Texas M. D. Anderson Cancer Center, Houston, TX 77030, USA; [7]Department of Epidemiology, Richard M. Fairbanks School of Public Health, Indiana University, Indianapolis, IN 46202, USA; [8]Department of Dermatology, Rhode Island Hospital, Providence, RI 02901, USA; [9]Warren Alpert Medical School at Brown University, Providence, RI 02901, USA; [10]The Channing Division of Network Medicine, Department of Medicine, Brigham and Women's Hospital, Harvard Medical School, Boston, MA 02115, USA; [11]Department of Medicine, Duke University School of Medicine, Durham, NC 27710, USA

Received September 14, 2020; Accepted December 7, 2020; Epub June 15, 2021; Published June 30, 2021

Abstract: Both *in vivo* and *in vitro* evidence has supported a key role of myeloid cells in immune suppression in melanoma and in promoting melanocytic metastases. Some single-nucleotide polymorphisms (SNPs) have been shown to predict cutaneous melanoma-specific survival (CMSS), but the association between genetic variation in myeloid cell-related genes and cutaneous melanoma (CM) patient survival remains unknown. Methods: we investigated associations between SNPs in myeloid cell-related pathway genes and CMSS in a discovery dataset of 850 CM patients and replicated the findings in another dataset of 409 CM patients. Results: we identified two SNPs (*EML1* rs10151787 A>G and *HIST1H4E* rs2069018 T>C) as independent prognostic factors for CMSS, with adjusted allelic hazards ratios of 1.56 (95% confidence interval =1.19-2.05, *P*=0.001) and 1.66 (1.22-2.26, *P*=0.001), respectively; so were their combined unfavorable alleles in a dose-response manner in both discovery and replication datasets (P_{trend}<0.001 and 0.002, respectively). Additional functional analysis revealed that both *EML1* rs10151787 G and *HIST1H4E* rs2069018 C alleles were associated with elevated mRNA expression levels in normal tissues. Conclusions: Our findings suggest that *EML1* rs10151787 A>G and *HIST1H4E* rs2069018 T>C are independent prognostic biomarkers for CMSS.

Keywords: Cutaneous melanoma, myeloid cell, single-nucleotide polymorphism, survival, prognostic factors

Introduction

Cutaneous melanoma (CM) is one of the most aggressive skin malignancies, with more than 100,000 new cases and 6,850 deaths estimated in 2020 in the United States [1]. Despite significant advances in the treatment of CM in the previous decade, CM-specific survival (CMSS) varies greatly and is hardly predicted accurately in patients with CM of any stage, partly due to the high metastatic potential of CM [2, 3]. Although some clinical predictors for CM survival exist, identification of additional prognostic factors for metastatic CMSS could offer more precision in treatment decisions for CM patients.

Increasing evidence has shown that pre-metastatic tumor microenvironment, consisting mainly of myeloid cells, is critical for tumor cell recruitment and survival to facilitate metastasis [4-8]. Myeloid cells were recently found to suppress dendritic cell differentiation and $CD8^+$ T cell proliferation, thus promoting the growth of B16F10 melanoma cells and lung metastasis [9]. Another study showed that myeloid cell accumulation in pre-metastatic tissues suppressed the anti-tumor cytotoxicity of tumor-

specific $CD8^+$ T cells in mouse models of melanoma and a significant increase in myeloid cells in the histopathology of metastasis-negative sentinel lymph nodes from melanoma patients [10]. Furthermore, specific myeloid cells were found to be expanded in melanoma patients treated with dendritic cell vaccines, causing enhanced PD-L1 expression as well as hindering $CD4^+$ T cell proliferation [11]. Since these studies obviously support a prominent role of myeloid cells in driving melanoma cell metastases in both *in vivo* and *in vitro* models, we believe myeloid cells may serve as a prognostic marker for CM patient survival.

However, myeloid cell markers are seldom cell-type specific and vary considerably across different cancer tissues [12], making accurate detection of myeloid cells in CM patient tissue difficult [13]; therefore, there have been few studies on associations between myeloid cells and CM patient survival. Recent studies suggest that single-nucleotide polymorphisms (SNPs) may be useful biomarkers for tumor progression and patient survival [14, 15], which implies that genetic variation could be a prognostic factor for CMSS. For example, studies have identified some specific SNPs as targeting molecules involved in melanoma pathogenesis, consequently controlling melanoma progress and patient outcomes [16-18].

Although several genome-wide association studies (GWASs) have identified some susceptibility loci for CM [19-21], few functional SNPs have been reported to be associated with CMSS at the GWAS level [22, 23]. An alternative approach is a novel hypothesis-driven post-GWAS strategy that uses available genotyping data to identify functional genetic variants in the targeted biological pathway genes and reveal their associations with CMSS at a pathway level [24, 25]. Therefore, to explore the value of myeloid cells in the prognosis of CMSS, we hypothesize that genetic variants of myeloid cell-related pathway genes are associated with CMSS, and we verified this hypothesis using two publically available CM GWAS datasets in the present study.

Materials and methods

Study populations

The discovery group derived from The University of Texas MD Anderson Cancer Center (MDACC) CM GWAS study that comprised genotyping and outcome data on 858 non-Hispanic white CM patients. The replication group used data on an additional 409 white participants from CM GWAS datasets in the Nurses' Health Study (NHS) and Health Professionals Follow-up Study (HPFS). Participant selection and data collection for both discovery and replication groups have been published in detail elsewhere [20, 26]. All the subjects in the present study provided a written informed consent under a protocol approved by the Institutional Review Boards of the MDACC, Brigham and Women's Hospital, and the Harvard T.H. Chan School of Public Health, and those of participating registries as required.

Gene selection

Based on the Molecular Signatures Database of the Gene Set Enrichment Analysis (GSEA) website, we comprehensively extracted 280 myeloid cell-related pathway genes located only on the autosomes (Supplementary Table 1).

SNP genotyping

The genotyping of DNA samples in both the discovery MDACC dataset and the NHS/HPFS replication datasets are detailed in Supplementary Methods.

Statistical methods

The details of statistical analyses are presented in Supplementary Methods.

Results

Baseline characteristics of study populations

The baseline characteristics of CM patients from the MDACC and NHS/HPFS datasets are described in Supplementary Table 2. CM patients from the MDACC dataset were between 17 and 94 years of age with a mean age of 52.4 (± 14.4) years at diagnosis, of whom 82.6% had stage I/II CM; the median follow-up time was 81.1 months with 95 CM-related deaths. CM patients from the NHS/HPFS dataset were between 34 and 87 years of age with a mean age of 61.1 (± 10.8) years at diagnosis; the median follow-up time was 179.0 months, and the mortality rate was 11.7%. There were no associations between principal components in

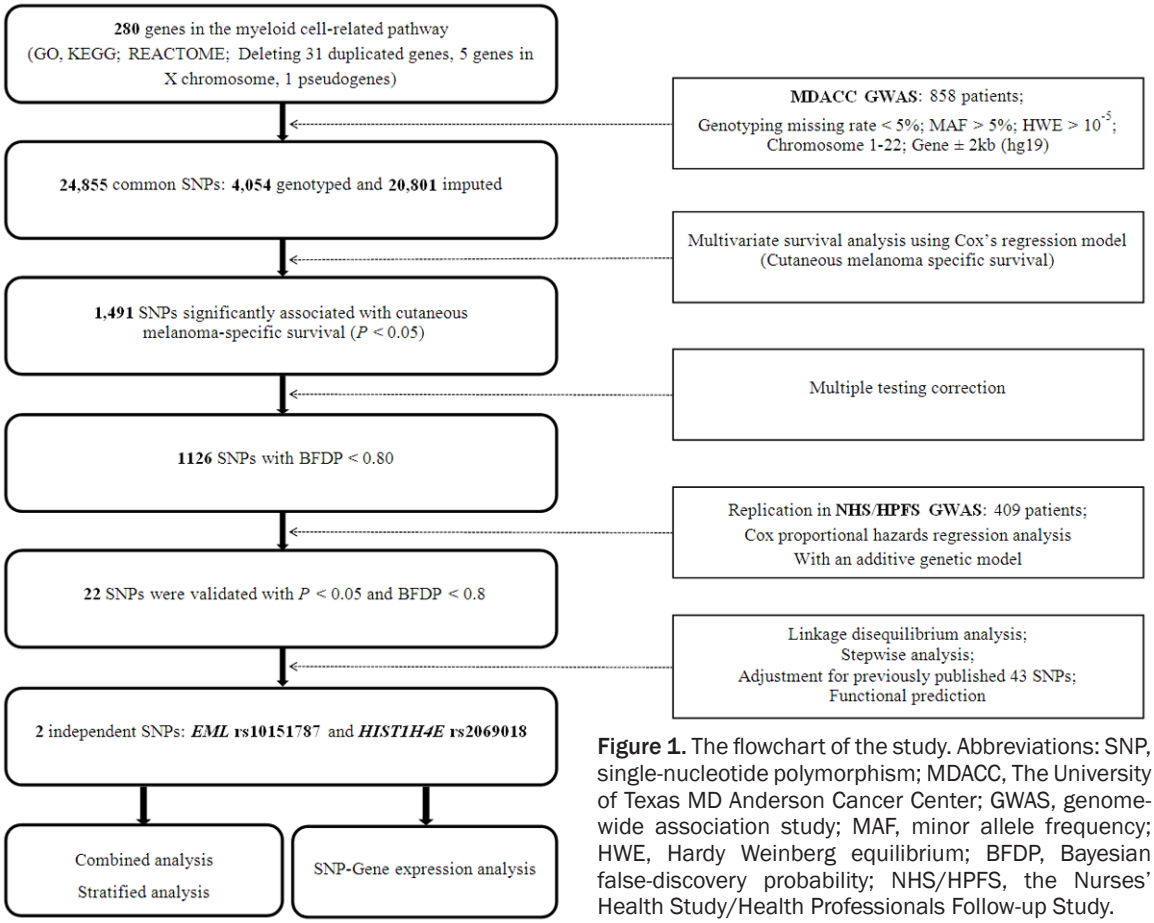

Figure 1. The flowchart of the study. Abbreviations: SNP, single-nucleotide polymorphism; MDACC, The University of Texas MD Anderson Cancer Center; GWAS, genome-wide association study; MAF, minor allele frequency; HWE, Hardy Weinberg equilibrium; BFDP, Bayesian false-discovery probability; NHS/HPFS, the Nurses' Health Study/Health Professionals Follow-up Study.

GWAS datasets and CM survival in these datasets; therefore, there was unnecessary to adjust for principal components.

Associations between SNPs in myeloid cell-related pathway genes and CMSS in the MDACC and NHS/HPFS datasets

An overall flowchart of the present study is presented in **Figure 1**. We first explored the associations between all acquired SNPs (including 4,054 genotyped and 20,801 imputed SNPs) in 280 myeloid cell-related pathway genes with CMSS in the MDACC dataset and found that 1126 SNPs were associated with CMSS (P<0.05) in an additive model with multiple test correction. After replication in the NHS/HPFS dataset, only 22 SNPs remained significant. These 22 SNPs are located in seven genes, i.e., three SNPs in *WNT2B* (Wnt family member 2B), three SNPs in *HIST1H4D* (histone cluster 1), eight SNPs in *HIST1H4E* (H4 clustered histone 5), two SNPs in *HIST1H4F* (H4 clustered histone 6), one SNP in *ARL11* (ADP ribosylation factor like GTPase 11), one SNP in *EML1* (echinoderm microtubule-associated protein-like 1), and four SNPs in *UBASH3B* (ubiquitin-associated and SH3 domain containing B) (Supplementary Table 3).

Two SNPs independently predict CMSS

To detect SNPs that are independently associated with CMSS, we first performed stepwise multivariable Cox regression analyses to assess the effects of our 22 validated SNPs on CMSS in the MDACC dataset. Four SNPs (rs1175649 in *WNT2B*, rs2069018 in *HIST1H4E*, rs61959910 in *ARL11*, and rs10151787 in *EML1*) remained significantly associated with CMSS (P<0.05) in the presence of clinical covariates (i.e., age, sex, Breslow thickness of tumor, regional/distant metastasis, mitotic rate, and ulceration). We then expanded this survival model by including 43 previously reported SNPs in the MDACC GWAS dataset; finally we found that two SNPs (*EML1* rs10151787 A>G and *HIST1H4E* rs2069018

Table 1. Two independent SNPs identified by multivariate Cox proportional hazards regression analysis including the selected variables and previously published survival-associated SNPs in the MDACC dataset

Variables[1]	Category[2]	Frequency	HR (95% CI)[1]	*P*[1]	HR (95% CI)[3]	*P*[3]
Age	≤50/>50	371/487	1.02 (1.00-1.04)	0.007	1.04 (1.02-1.06)	<.0001
Sex	Female/Male	362/496	1.49 (0.93-2.37)	0.096	1.35 (0.79-2.29)	0.269
Regional/distant metastasis	No/Yes	709/149	3.93 (2.54-6.06)	<0.0001	12.00 (6.63-21.72)	<.0001
Breslow thickness (mm)	≤1/>1	347/511	1.19 (1.12-1.26)	<0.0001	1.25 (1.15-1.35)	<.0001
Ulceration	No/Yes	681/155	3.04 (1.95-4.76)	<0.0001	5.08 (2.90-8.91)	<.0001
Mitotic rate (mm^2)	≤1/>1	275/583	2.32 (1.13-4.75)	0.022	2.30 (0.99-5.36)	0.053
EML1 rs10151787 A>G	AA/AG/GG	509/311/38	1.56 (1.11-2.18)	0.010	1.64 (1.09-2.48)	0.018
HIST1H4E rs2069018 T>C	TT/TC/CC	636/204/18	1.51 (1.03-2.22)	0.036	2.28 (1.39-3.73)	0.001

Abbreviations: SNP, single-nucleotide polymorphism; MDACC, The University of Texas MD Anderson Cancer Center; HR, hazards ratio; CI, confidence interval. [1]Stepwise analysis included age, sex, regional/distant metastasis, Breslow thickness, ulceration, mitotic rate and 22 validated SNPs; [2]The "category/" was used as the reference; [3]Published SNPs were used for post-stepwise adjustment: rs1175649, rs1124379, rs10916352, rs6707820, rs6750552, rs6785564, rs2306574, rs11551405, rs1718404, rs12512631, rs788935, rs32579, rs3734398, rs7826362, rs10090371, rs7850212, rs3851552, rs10882807, rs61873997, rs35748949, rs11018104, rs7944031, rs11037684, rs508485, rs7933369, rs11225163, rs1990330, rs7953425, rs2342924, rs10846684, rs206118, rs10492396, rs3752447, rs2596191, rs782917, rs17204952, rs62068372, rs72635537, rs7253062, rs3918251, rs12663017, rs17676826, rs8012548.

T>C) remained significantly associated with CMSS (*P*=0.018 and 0.001, respectively) (**Table 1**). The results of our meta-analysis of these two independent SNPs in each dataset are presented in **Table 2**, showing the absence of heterogeneity across these datasets.

Furthermore, as shown in **Table 3**, we noticed that the *EML1* rs10151787 G allele and the *HIST1H4E* rs2069018 C allele were prognostic risk alleles for CMSS in the MDACC dataset (P_{trend}=0.017 and 0.012, respectively) with similar results in both the NHS/HPFS dataset (P_{trend}=0.033 and 0.042, respectively) and the combined MDACC and NHS/HPFS dataset (P_{trend}=0.0004 and 0.006, respectively). All of the SNPs investigated in the present study are depicted in a Manhattan plot in Supplementary Figure 1, and regional association plots for these two independent SNPs are displayed in Supplementary Figure 2.

Combined risk alleles of two independent CMSS-associated SNPs

To identify the collective effect of *EML1* rs10151787 A>G and *HIST1H4E* rs2069018 T>C on CMSS, we combined their risk alleles (i.e., *EML1* rs10151787 G allele and *HIST1H4E* rs2069018 C allele) into one variable as a genetic score. Patients in each dataset were categorized into four groups (i.e., 0, 1, 2, and 3-4) according to their number of risk alleles (NRA), and the trend test in each dataset showed a significant risk-allele dose-response effect on CMSS. Specifically, higher NRA was associated with a worse survival in the MDACC dataset (P_{trend}=0.0008), the NHS/HPFS dataset (P_{trend}=0.002), and the combined MDACC and NHS/HPFS dataset (P_{trend}<0.0001) after adjustment for available covariates (**Table 3**). Moreover, we also dichotomized all CM patients into two groups: 0-1 or 2-4 NRA. As shown in **Table 3**, the 2-4 NRA group had a significantly worse CMSS in the MDACC dataset (HR=2.48; 95% CI=1.56-3.95, *P*=0.0001), compared with the 0-1 NRA group. Similarly, the 2-4 NRA group showed a significantly worse CMSS in the combined MDACC and NHS/HPFS dataset (HR=2.33; 95% CI=1.59-3.41, *P*<0.0001). Furthermore, we constructed Kaplan-Meier (KM) survival curves to display the associations between NRA and CMSS (**Figure 2A-C**).

Stratified analysis for the effect of NRA on the CMSS

To determine whether the impact of NRA on CMSS was modified by other available clinical covariates, we employed stratified analysis in both MDACC (clinical covariates including sex, age, ulceration, mitotic rate, distant/regional metastasis, ulceration, and Breslow thickness of tumor) and NHS/HPFS datasets (clinical variables including age and sex). In the MDACC dataset, compared with CM patients having 0-1 NRA, those with 2-4 NRA had a significantly poorer CMSS, except for the subgroup with stage III/IV, mitotic rate ≤1, and Breslow thick-

Table 2. Meta-analysis of the two independent SNPs in myeloid cell-related pathway genes

SNP	Allele[1]	Gene	Discovery-MDACC (n=858)				Replication-NHS/HPFS (n=409)				Combined-Meta-analysis (n=1267)			
			EAF	HR (95% CI)[2]	*P*[2]	BFDP[3]	EAF	HR (95% CI)[4]	*P*[4]	BFDP[3]	P_{het}	I^2	HR (95% CI)[5]	*P*[5]
rs10151787[6]	A>G	*EML1*	0.23	1.51 (1.07-2.11)	0.017	0.682	0.20	1.65 (1.04-2.61)	0.033	0.769	0.761	0	1.56 (1.19-2.05)	0.001
rs2069018[7]	T>C	*HIST1H4E*	0.14	1.64 (1.12-2.42)	0.012	0.631	0.13	1.70 (1.02-2.84)	0.042	0.798	0.913	0	1.66 (1.22-2.26)	0.001

Abbreviations: SNP, single-nucleotide polymorphism; GWAS, genome-wide association study; MDACC, The University of Texas MD Anderson Cancer Center; NHS/HPFS, the Nurses' Health Study/Health Professionals Follow-up Study; EAF, effect allele frequency; HR, hazards ratio; CI, confidence interval; BFDP, Bayesian false-discovery probability; P_{het}, *P* value for heterogeneity by Cochrane's Q test. [1]Reference allele>effect allele; [2]Adjusted for age, sex, Breslow thickness, distant/regional metastasis, ulceration and mitotic rate in an additive genetic model; [3]BFDP was used for multiple test correction with detected a highest HR of 2.0 and a prior probability of 0.1; [4]Adjusted for age and sex in an additive genetic model; [5]Meta-analysis in a fix-effects model; [6]Imputed SNP in the MDACC GWAS dataset; [7]Genotyped SNP in the MDACC GWAS dataset.

Table 3. Associations between the two identified independent SNPs in myeloid cell-related pathway genes and CMSS of patients in the MDACC dataset, the NHS/HPFS dataset and the combined dataset

Genotype	MDACC (n=858)				NHS/HPFS (n=409)				MDACC + NHS/HPFS (n=1267)			
	Frequency		Multivariate analysis[1]		Frequency		Multivariate analysis[2]		Frequency		Multivariate analysis[3]	
	All	Death (%)	HR (95% CI)	*P*	All	Death (%)	HR (95% CI)	*P*	All	Death (%)	HR (95% CI)	*P*
EML1 rs10151787 A>G												
AA	509	44 (8.64)	1.00		262	24 (9.16)	1.00		771	68 (8.82)	1.00	
AG	311	45 (14.47)	1.55 (1.01-2.38)	0.045	134	22 (16.42)	1.93 (1.08-3.45)	0.026	445	67 (15.06)	1.81 (1.29-2.53)	<0.001
GG	38	6 (15.79)	2.13 (0.89-5.11)	0.089	13	2 (15.38)	1.81 (0.43-7.67)	0.423	51	8 (15.69)	2.03 (0.97-4.22)	0.059
Trend test				0.017				0.033				<0.001
HIST1H4E rs2069018 T>C												
TT	636	64 (10.06)	1.00		309	32 (10.36)	1.00		945	96 (10.16)	1.00	
TC	204	28 (13.73)	1.60 (1.01-2.52)	0.045	92	13 (14.13)	1.34 (0.71-2.57)	0.369	296	41 (13.85)	1.41 (0.98-2.03)	0.066
CC	18	3 (16.67)	3.03 (0.93-9.85)	0.066	8	3 (37.50)	5.08 (1.55-16.62)	0.007	26	6 (23.08)	2.97 (1.30-6.78)	0.010
Trend test				0.012				0.042				0.006
Number of combined risk alleles[4]												
0	377	33 (8.75)	1.00		193	13 (6.74)	1.00		570	46 (8.07)	1.00	
1	359	36 (10.03)	1.22 (0.75-1.99)	0.431	167	26 (15.57)	2.35 (1.20-4.57)	0.012	526	62 (11.79)	1.54 (1.05-2.25)	0.027
2	100	23 (23.00)	2.82 (1.63-4.87)	<0.001	46	8 (17.39)	2.95 (1.22-7.16)	0.016	146	31 (21.23)	3.00 (1.90-4.73)	<.0001
3-4	22	3 (13.64)	2.21 (0.67-7.31)	0.195	3	1 (33.33)	6.86 (0.89-53.00)	0.065	25	4 (16.00)	2.38 (0.85-6.64)	0.098
Trend test				<0.001				0.002				<.0001
0-1	736	69 (9.38)	1.00		360	39 (10.83)	1.00		1096	108 (9.85)	1.00	
2-4	122	26 (21.31)	2.48 (1.56-3.95)	<0.001	49	9 (18.37)	1.95 (0.94-4.06)	0.073	171	35 (20.47)	2.33 (1.59-3.41)	<.0001

Abbreviations: SNP, single-nucleotide polymorphism; CMSS, cutaneous melanoma-specific survival; MDACC, The University of Texas MD Anderson Cancer Center; NHS/HPFS, the Nurses' Health Study/Health Professionals Follow-up Study; HR, hazards ratio; CI, confidence interval. [1]Adjusted for age, sex, Breslow thickness, distant/regional metastasis, ulceration and mitotic rate in Cox models of SNPs and CMSS in MDACC study; [2]Adjusted for age and sex in Harvard NHS/HPFS study; [3]Adjusted for age and sex in MDACC and Harvard NHS/HPFS study. [4]Risk alleles include *EML1* rs10151787 G allele and *HIST1H4E* rs2069018 C allele.

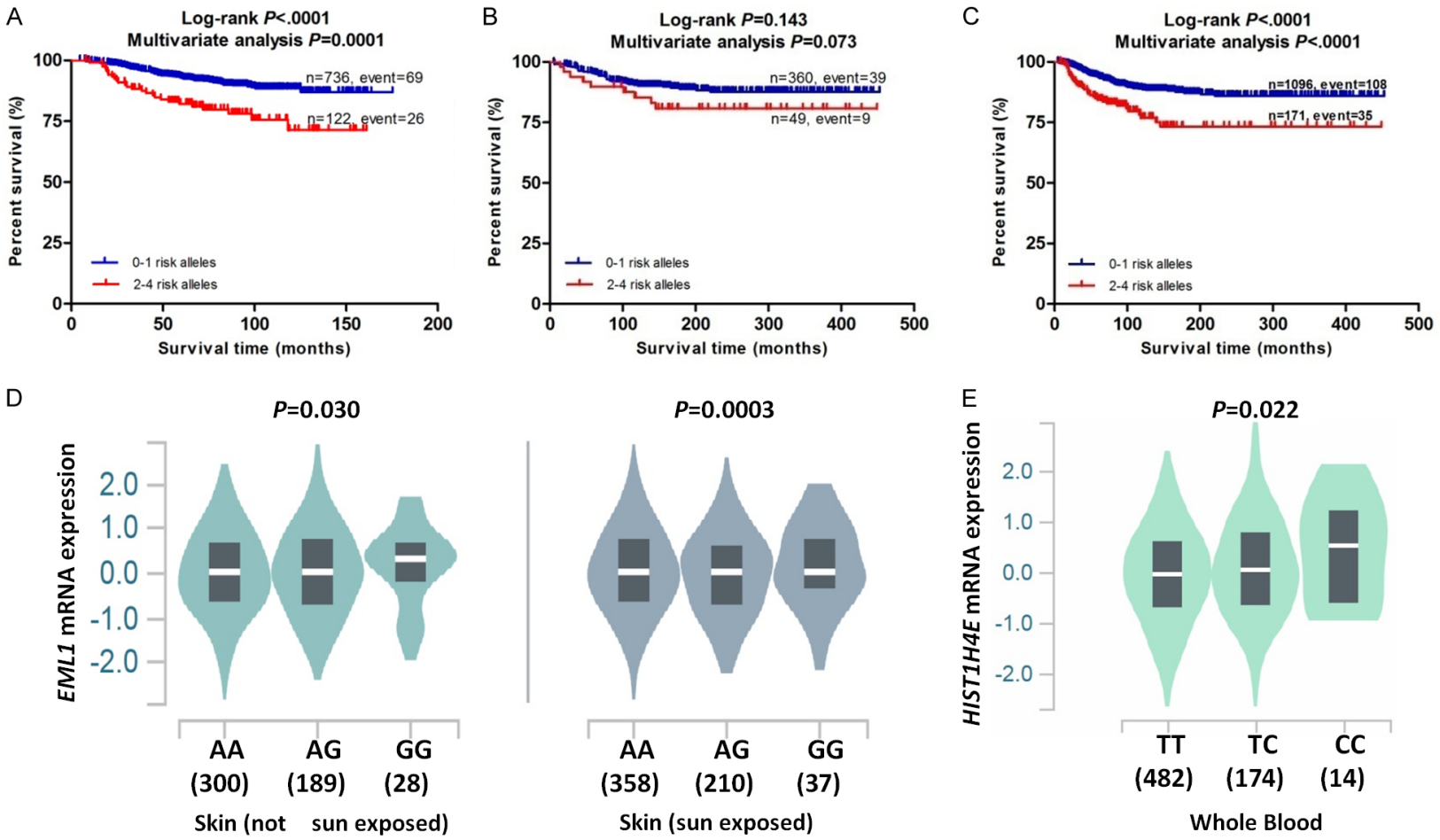

Figure 2. Two independent SNPs in myeloid cell-related pathway genes predict cutaneous melanoma survival and eQTL analysis for them. Kaplan-Meier survival curves of combined risk alleles of *EML1* rs10151787 and *HIST1H4E* rs2069018 on CMSS: dichotomized 0-1 risk allele group and 2-4 risk alleles group in the MDACC dataset (A), the NHS/HPFS dataset (B) and the combined MDACC and NHS/HPFS dataset (C). The correlation of rs10151787 genotypes and *EML1* mRNA expression in skin tissues from the GTEx (D). The correlation of rs2069018 and *HIST1H4E* mRNA expression in whole blood samples from the GTEx (E). Abbreviations: SNP, single-nucleotide polymorphism; eQTL, expression quantitative trait loci; CMSS, cutaneous melanoma-specific survival; MDACC, The University of Texas MD Anderson Cancer Center; NHS, the Nurses'Health Study; HPFS, the Health Professionals Follow-up Study; GTEx, Genotype-Tissue Expression project.

ness ≤1 mm. No significant effects of interaction between risk alleles and each covariate on CMSS were found in these datasets (Supplementary Table 4).

Receiver operating characteristic (ROC) curves and time-dependent area under receiver curve (AUC) of the two independent SNPs for CMSS prediction

To further explore the predictive value of *EML1* rs10151787 A>G and *HIST1H4E* rs2069018 T>C, time-dependent AUC and ROC curves were designed for CM patients in the presence of available clinical covariates. In the MDACC dataset, although the time-dependent AUC in the model with clinical variables increased from 79.02% to 79.51% when risk alleles (i.e., *EML1* rs10151787 G allele and *HIST1H4E* rs2069018 C allele) were added, the predictive performance of 5-year CMSS ROC curves did not significantly improve (P=0.752) (Supplementary Figure 3A, 3B). In the NHS/HPFS dataset, the predictive performance of 5-year CMSS ROC curves in the model with clinical covariables was dramatically improved by adding risk SNPs (P=1.46×10^{-4}), and the time-dependent AUC increased from 54.05% to 73.27% (Supplementary Figure 3C, 3D). Finally, in the combined MDACC and NHS/HPFS datasets, the predictive performance of 5-year CMSS ROC curves in the model with common clinical variables (age, sex) did not significantly improve (P=0.119) (Supplementary Figure 3E, 3F).

Functional predictions of the two SNPs

To investigate specific biological functions of *EML1* rs10151787 A>G and *HIST1H4E* rs2069018 T>C associated with CMSS, we explored SNP-related genomics data using an online bioinformatics tool (HaploReg). We found that an A>G change in *EML1* rs10151787 may disturb protein motifs. In addition, a T>C change in *HIST1H4E* rs2069018 was predicted to be located at a promoter histone marker region or DNAse region, which may also disturb protein motifs, while other identified significant SNPs showing a high linkage disequilibrium (LD) ($r^2 \geq 0.8$) with rs2069018 may be involved in regulating expression of histone in specific regions, DNase expression, and protein binding (Supplementary Table 3). Using data extracted from the Encyclopedia of DNA Elements (ENCODE) project, we found that rs10151787 was probably located on the H3K4Me1 motifs, while rs2069018 was highly probably located on the H3K27Ac, H3K4Me3, and H3K4Me1 motifs (Supplementary Figure 4). These findings suggest a strong possibility that *EML1* rs10151787 A>G and *HIST1H4E* rs2069018 T>C may disturb their gene's expression through transcriptional regulation.

Two independent SNPs regulate their corresponding mRNA expression

To further investigate molecular mechanisms underlying the associations between two independent SNPs and CMSS, we explored correlations between risk alleles (i.e., *EML1* rs10151787 G allele and *HIST1H4E* rs2069018 C allele) and their corresponding mRNA expression levels by the expression quantitative trait loci (eQTL) analysis. In the RNA-Seq data from the 1000 Genomes Project, the rs10151787 G allele showed no correlation with *EML1* mRNA expression in any additive, dominant, or recessive model (Supplementary Figure 5A-C); no *HIST1H4E* mRNA expression data were available in the 1000 Genomes Project. Additionally, we also extracted data from the genotype-tissue expression (GTEx) Project, and the results showed that the rs10151787 G allele was significantly associated with increased *EML* mRNA expression in normal tissues from sun-exposed lower leg skin (P=0.0003) and unexposed suprapubic skin (P=0.03) (**Figure 2D**). Meanwhile, the rs2069018 C allele was significantly correlated with higher *HIST1H4E* mRNA expression levels in normal whole blood samples (P=0.022) (**Figure 2E**) but not in normal skin tissues (Supplementary Figure 5D).

Finally, we measured mRNA expression of *EML* and *HIST1H4E* in 104 primary CM tissues and 368 metastatic CM tissues available from the The Cancer Genome Atlas (TCGA) database. As shown in Supplementary Figure 6A and 6C, mRNA expression levels of *EML* and *HIST1H4E* were both significantly higher in metastatic CM tissues (P=0.003 and P=0.045, respectively) than in primary CM tissues. However, as displayed by KM survival curves in Supplementary Figure 6B and 6D, mRNA expression levels of both *EML* and *HIST1H4E* were not associated with CM survival in the TCGA database.

Discussion

In the present study, we investigated the associations between 24,855 SNPs of 280 myeloid cell-related pathway genes and CMSS using available genotyping and clinical outcome data from two previously reported CM GWAS datasets. We identified two SNPs (*EML1* rs10151787 A>G and *HIST1H4E* rs2069018 T>C) that were independently associated with CMSS. In addition, we found that the rs10151787 G allele was associated with significantly increased *EML1* mRNA expression, while the rs2069018 C allele was associated with significantly increased *HIST1H4E* mRNA expression. Furthermore, our results revealed that mRNA expression levels of both *EML1* and *HIST1H4E* were increased in CM metastatic tissues. In addition, these two SNPs were independent of other clinical characteristics of tumors including tumor thickness, presence of ulceration, and distant metastases in both the MDACC and the NHS/HPFS datasets. Therefore, the present study of 1267 Caucasian CM patients identified two SNPs as independently prognostic predictors for CMSS.

Metastasis is the major cause of mortality in CM patients, and tumor-infiltrating myeloid cells are the key component of the tumor microenvironment, likely involved in melanoma cell metastasis [9, 10]. Notably, the presence of tumor-infiltrating myeloid cells in melanoma tumors has been reportedly to be correlated with melanoma patient survival [27], implying that functions of myeloid cells could be a prognostic marker for melanoma patient survival. However, myeloid cells are a highly diverse population, including various cellular subtypes and lacking cell-type specific markers [13, 28, 29]; hence, accurately assessing functions of myeloid cells in CM tumor tissue and further addressing their correlations with CM survival remains difficult. In the present study, we explored the prognostic value of genetic surrogates for functions of myeloid cells in CM by analyzing associations between SNPs in myeloid cell-related pathway genes and CMSS, instead of directly detecting the presence of myeloid cells in CM tissue. Given the accuracy of *EML1* rs10151787 A>G and *HIST1H4E* rs2069018 T>C in predicting CMSS in the present study, our results may provide easily detectable biomarkers for survival of CM patients, if validated by other investigators.

To date, however, no published studies have reported an association between *EML1* or *HIST1H4E* and CM patient survival. *EML1*, also known as echinoderm microtubule-associated protein-like 1, has been identified as playing an important role in regulating molecular mechanisms underlying neuronal localization and normal cortical development [30]. Mutations in *Eml1* have been shown to cause ectopic progenitors and neuronal heterotopia in both mouse models and human tissues [31]. Few studies have investigated the roles of *EML1* in CM. One recent study suggested that *EML1* fused with *ABL1* might serve as a tyrosine kinase, because it induced myeloid cell transformation [32]. To our knowledge, the present study is the first to report an association between genetic variants of *EML1* and CM survival. In addition, *EML1* rs10151787 A>G showed a significant risk effect on CMSS and a significant association with elevated *EML1* mRNA expression levels in normal skin tissues; furthermore, *EML1* mRNA conspicuously accumulated in metastatic CM tissues, compared with primary CM tissues. These observations suggest that *EML1* may serve as an oncogene in CM.

HIST1H4E, also called H4 clustered histone 5, is a member of the histone H4 family. Several histone variants have been confirmed as key epigenetic players implicated in the regulation of cancer progression [33]. Studies have linked changes in the global expression of some histones to melanoma metastasis [34, 35]. However, no direct implication of *HIST1H4E* in melanoma has been reported. In the present study, we found that *HIST1H4E* rs2069018 T>C, a risk factor for CMSS, was associated with an elevated *HIST1H4E* mRNA expression in normal whole blood, while, *HIST1H4E* mRNA expression was significantly elevated in metastatic CM tissues, compared with primary CM tissues. Therefore, rs2069018 C allele-regulated *HIST1H4E* mRNA expression may be a molecular mechanism underlying the observed association between *HIST1H4E* rs2069018 and poor survival in CM patients.

In addition to these above-mentioned findings, these are some limitations in the present study. The CM patients were recruited only from Caucasian populations; thus, further validation of CM patient cohorts in different races/ethnicities should be conducted. Additionally, com-

pared with the MDACC discovery dataset, fewer CM participants with a small number of clinical covariates were enrolled in the NHS/HPFS replication dataset, which could weaken statistical power in validating the effects of other SNPs identified in the discovery dataset. Finally, the sample sizes of CM patients from these two datasets were not large enough to perform the false discovery rate test; however, considering that up to 83% of selected SNPs in the present study were imputed, the Bayesian false-discovery probability test might be more appropriate for the highly correlated SNPs.

Overall, myeloid cells have been shown to be involved in melanoma progression, and pathologists have tried to determine whether the presence of myeloid cells predicts CM patient outcomes. Given the potential prognostic value of *EML1* rs10151787 A>G and *HIST1H4E* rs2069018 T>C in myeloid cell-related pathway genes in predicting CMSS, as the AUC was not statistically significant, additional causal SNPs need to be identified in larger studies. These two SNPs may serve either as a new prognostic biomarker or as a precision clinical treatment indicator for CM patients and their caregivers, once these findings are validated in future studies.

Acknowledgements

The authors would like to thank Bingrong Zhou and Guiqing Lu for their technical assistance and all participants and staff members of the Nurses' Health Study and Health Professionals Follow-Up Study for their valuable contributions as well as the following state cancer registries for their support: AL, AZ, AR, CA, CO, CT, DE, FL, GA, ID, IL, IN, IA, KY, LA, ME, MD, MA, MI, NE, NH, NJ, NY, NC, ND, OH, OK, OR, PA, RI, SC, TN, TX, VA, WA, WY. The authors also thank the Channing Division of Network Medicine, Department of Medicine, Brigham and Women's Hospital, for its support as home of the NHS, Harvard Medical School. The authors assume full responsibility for analyses and interpretation of these data. We also thank the John Hopkins University Center for Inherited Disease Research for conducting high-throughput genotyping for our study. The results published herein are fully or partly based upon data from the TCGA pilot project established by the NCI and NHGRI. Information about TCGA and the investigators and institutions that constitute the TCGA research network can be found at http://cancergenome.nih.gov. We also thank all of the investigators and funding agencies that enabled the deposition of data in dbGaP that we used in this study (dbGaP Study Accession: phs000187.v1.p1). This work was supported by NIH/NCI R01 CA100264, 2P50CA093459, R01CA133996, R01 CA49449, P01 CA87969, UM1 CA186107, U01 CA167552, The University of Texas MD Anderson Cancer Center Various Donors Melanoma and Skin Cancers Priority Program Fund, the Miriam and Jim Mulva Research Fund, the McCarthy Skin Cancer Research Fund, and the Marit Peterson Fund for Melanoma Research. Qingyi Wei was partly supported by start-up funds from Duke Cancer Institute, Duke University Medical Center, and Duke Cancer Institute as part of the P30 Cancer Center Support Grant (Grant ID: NIH CA014236).

Disclosure of conflict of interest

None.

Address correspondence to: Dr. Qingyi Wei, Duke Cancer Institute, Duke University Medical Center, 905 South LaSalle Street, Durham 27710, North Carolina, USA. Tel: 919-660-0562; E-mail: qingyi.wei@duke.edu

References

[1] Siegel RL, Miller KD and Jemal A. Cancer statistics, 2020. CA Cancer J Clin 2020; 70: 7-30.

[2] Schadendorf D, van Akkooi ACJ, Berking C, Griewank KG, Gutzmer R, Hauschild A, Stang A, Roesch A and Ugurel S. Melanoma. Lancet 2018; 392: 971-984.

[3] Enninga EAL, Moser JC, Weaver AL, Markovic SN, Brewer JD, Leontovich AA, Hieken TJ, Shuster L, Kottschade LA, Olariu A, Mansfield AS and Dronca RS. Survival of cutaneous melanoma based on sex, age, and stage in the United States, 1992-2011. Cancer Med 2017; 6: 2203-2212.

[4] Jian J, Pang Y, Yan HH, Min Y, Achyut BR, Hollander MC, Lin PC, Liang X and Yang L. Platelet factor 4 is produced by subsets of myeloid cells in premetastatic lung and inhibits tumor metastasis. Oncotarget 2017; 8: 27725-27739.

[5] Lim SY, Gordon-Weeks A, Allen D, Kersemans V, Beech J, Smart S and Muschel RJ. Cd11b(+) myeloid cells support hepatic metastasis through down-regulation of angiopoietin-like 7 in cancer cells. Hepatology 2015; 62: 521-533.

[6] Hirai H, Fujishita T, Kurimoto K, Miyachi H, Kitano S, Inamoto S, Itatani Y, Saitou M, Maeka-

wa T and Taketo MM. CCR1-mediated accumulation of myeloid cells in the liver microenvironment promoting mouse colon cancer metastasis. Clin Exp Metastasis 2014; 31: 977-989.

[7] Kitamura T, Fujishita T, Loetscher P, Revesz L, Hashida H, Kizaka-Kondoh S, Aoki M and Taketo MM. Inactivation of chemokine (C-C motif) receptor 1 (CCR1) suppresses colon cancer liver metastasis by blocking accumulation of immature myeloid cells in a mouse model. Proc Natl Acad Sci U S A 2010; 107: 13063-13068.

[8] Itatani Y, Kawada K, Fujishita T, Kakizaki F, Hirai H, Matsumoto T, Iwamoto M, Inamoto S, Hatano E, Hasegawa S, Maekawa T, Uemoto S, Sakai Y and Taketo MM. Loss of SMAD4 from colorectal cancer cells promotes CCL15 expression to recruit CCR1+ myeloid cells and facilitate liver metastasis. Gastroenterology 2013; 145: 1064-1075, e1011.

[9] Papaspyridonos M, Matei I, Huang Y, do Rosario Andre M, Brazier-Mitouart H, Waite JC, Chan AS, Kalter J, Ramos I, Wu Q, Williams C, Wolchok JD, Chapman PB, Peinado H, Anandasabapathy N, Ocean AJ, Kaplan RN, Greenfield JP, Bromberg J, Skokos D and Lyden D. Id1 suppresses anti-tumour immune responses and promotes tumour progression by impairing myeloid cell maturation. Nat Commun 2015; 6: 6840.

[10] Zhang W, Zhang C, Li W, Deng J, Herrmann A, Priceman SJ, Liang W, Shen S, Pal SK, Hoon DSB and Yu H. CD8+ T-cell immunosurveillance constrains lymphoid premetastatic myeloid cell accumulation. Eur J Immunol 2015; 45: 71-81.

[11] Bakdash G, Buschow SI, Gorris MA, Halilovic A, Hato SV, Skold AE, Schreibelt G, Sittig SP, Torensma R, Duiveman-de Boer T, Schroder C, Smits EL, Figdor CG and de Vries IJ. Expansion of a BDCA1+CD14+ myeloid cell population in melanoma patients may attenuate the efficacy of dendritic cell vaccines. Cancer Res 2016; 76: 4332-4346.

[12] Engblom C, Pfirschke C and Pittet MJ. The role of myeloid cells in cancer therapies. Nat Rev Cancer 2016; 16: 447-462.

[13] Gunther P and Schultze JL. Mind the map: technology shapes the myeloid cell space. Front Immunol 2019; 10: 2287.

[14] Van den Broeck T, Joniau S, Clinckemalie L, Helsen C, Prekovic S, Spans L, Tosco L, Van Poppel H and Claessens F. The role of single nucleotide polymorphisms in predicting prostate cancer risk and therapeutic decision making. Biomed Res Int 2014; 2014: 627510.

[15] Zienolddiny S and Skaug V. Single nucleotide polymorphisms as susceptibility, prognostic, and therapeutic markers of nonsmall cell lung cancer. Lung Cancer (Auckl) 2012; 3: 1-14.

[16] Glatthaar H, Katto J, Vogt T and Mahlknecht U. Estrogen receptor alpha (ESR1) single-nucleotide polymorphisms (SNPs) affect malignant melanoma susceptibility and disease course. Genet Epigenet 2016; 8: 1-6.

[17] Figl A, Scherer D, Nagore E, Bermejo JL, Dickes E, Thirumaran RK, Gast A, Hemminki K, Kumar R and Schadendorf D. Single nucleotide polymorphisms in DNA repair genes XRCC1 and APEX1 in progression and survival of primary cutaneous melanoma patients. Mutat Res 2009; 661: 78-84.

[18] Onken MD, Worley LA, Person E, Char DH, Bowcock AM and Harbour JW. Loss of heterozygosity of chromosome 3 detected with single nucleotide polymorphisms is superior to monosomy 3 for predicting metastasis in uveal melanoma. Clin Cancer Res 2007; 13: 2923-2927.

[19] Barrett JH, Iles MM, Harland M, Taylor JC, Aitken JF, Andresen PA, Akslen LA, Armstrong BK, Avril MF, Azizi E, Bakker B, Bergman W, Bianchi-Scarra G, Bressac-de Paillerets B, Calista D, Cannon-Albright LA, Corda E, Cust AE, Debniak T, Duffy D, Dunning AM, Easton DF, Friedman E, Galan P, Ghiorzo P, Giles GG, Hansson J, Hocevar M, Hoiom V, Hopper JL, Ingvar C, Janssen B, Jenkins MA, Jonsson G, Kefford RF, Landi G, Landi MT, Lang J, Lubinski J, Mackie R, Malvehy J, Martin NG, Molven A, Montgomery GW, van Nieuwpoort FA, Novakovic S, Olsson H, Pastorino L, Puig S, Puig-Butille JA, Randerson-Moor J, Snowden H, Tuominen R, Van Belle P, van der Stoep N, Whiteman DC, Zelenika D, Han J, Fang S, Lee JE, Wei Q, Lathrop GM, Gillanders EM, Brown KM, Goldstein AM, Kanetsky PA, Mann GJ, Macgregor S, Elder DE, Amos CI, Hayward NK, Gruis NA, Demenais F, Bishop JA and Bishop DT; GenoMEL Consortium. Genome-wide association study identifies three new melanoma susceptibility loci. Nat Genet 2011; 43: 1108-1113.

[20] Amos CI, Wang LE, Lee JE, Gershenwald JE, Chen WV, Fang S, Kosoy R, Zhang M, Qureshi AA, Vattathil S, Schacherer CW, Gardner JM, Wang Y, Bishop DT, Barrett JH, Geno MELI, MacGregor S, Hayward NK, Martin NG, Duffy DL, Investigators QM, Mann GJ, Cust A, Hopper J, Investigators A, Brown KM, Grimm EA, Xu Y, Han Y, Jing K, McHugh C, Laurie CC, Doheny KF, Pugh EW, Seldin MF, Han J and Wei Q. Genome-wide association study identifies novel loci predisposing to cutaneous melanoma. Hum Mol Genet 2011; 20: 5012-5023.

[21] Bishop DT, Demenais F, Iles MM, Harland M, Taylor JC, Corda E, Randerson-Moor J, Aitken JF, Avril MF, Azizi E, Bakker B, Bianchi-Scarra G, Bressac-de Paillerets B, Calista D, Cannon-Al-

bright LA, Chin AWT, Debniak T, Galore-Haskel G, Ghiorzo P, Gut I, Hansson J, Hocevar M, Hoiom V, Hopper JL, Ingvar C, Kanetsky PA, Kefford RF, Landi MT, Lang J, Lubinski J, Mackie R, Malvehy J, Mann GJ, Martin NG, Montgomery GW, van Nieuwpoort FA, Novakovic S, Olsson H, Puig S, Weiss M, van Workum W, Zelenika D, Brown KM, Goldstein AM, Gillanders EM, Boland A, Galan P, Elder DE, Gruis NA, Hayward NK, Lathrop GM, Barrett JH and Bishop JA. Genome-wide association study identifies three loci associated with melanoma risk. Nat Genet 2009; 41: 920-925.

[22] Wang X, Tucker NR, Rizki G, Mills R, Krijger PH, de Wit E, Subramanian V, Bartell E, Nguyen XX, Ye J, Leyton-Mange J, Dolmatova EV, van der Harst P, de Laat W, Ellinor PT, Newton-Cheh C, Milan DJ, Kellis M and Boyer LA. Discovery and validation of sub-threshold genome-wide association study loci using epigenomic signatures. Elife 2016; 5: e10557.

[23] Hart AB and Kranzler HR. Alcohol dependence genetics: lessons learned from genome-wide association studies (GWAS) and post-GWAS analyses. Alcohol Clin Exp Res 2015; 39: 1312-1327.

[24] Gallagher MD and Chen-Plotkin AS. The post-GWAS era: from association to function. Am J Hum Genet 2018; 102: 717-730.

[25] Zhang X, Bailey SD and Lupien M. Laying a solid foundation for Manhattan--'setting the functional basis for the post-GWAS era'. Trends Genet 2014; 30: 140-149.

[26] Song F, Qureshi AA, Zhang J, Amos CI, Lee JE, Wei Q and Han J. Exonuclease 1 (EXO1) gene variation and melanoma risk. DNA Repair (Amst) 2012; 11: 304-309.

[27] Jensen TO, Schmidt H, Moller HJ, Donskov F, Hoyer M, Sjoegren P, Christensen IJ and Steiniche T. Intratumoral neutrophils and plasmacytoid dendritic cells indicate poor prognosis and are associated with pSTAT3 expression in AJCC stage I/II melanoma. Cancer 2012; 118: 2476-2485.

[28] Dress RJ, Dutertre CA, Giladi A, Schlitzer A, Low I, Shadan NB, Tay A, Lum J, Kairi M, Hwang YY, Becht E, Cheng Y, Chevrier M, Larbi A, Newell EW, Amit I, Chen J and Ginhoux F. Plasmacytoid dendritic cells develop from Ly6D(+) lymphoid progenitors distinct from the myeloid lineage. Nat Immunol 2019; 20: 852-864.

[29] Ruffell B and Coussens LM. Macrophages and therapeutic resistance in cancer. Cancer Cell 2015; 27: 462-472.

[30] Lyman KA and Chetkovich DM. Cortical compass: EML1 helps point the way in neuronal migration. Epilepsy Curr 2015; 15: 43-44.

[31] Kielar M, Tuy FP, Bizzotto S, Lebrand C, de Juan Romero C, Poirier K, Oegema R, Mancini GM, Bahi-Buisson N, Olaso R, Le Moing AG, Boutourlinsky K, Boucher D, Carpentier W, Berquin P, Deleuze JF, Belvindrah R, Borrell V, Welker E, Chelly J, Croquelois A and Francis F. Mutations in Eml1 lead to ectopic progenitors and neuronal heterotopia in mouse and human. Nat Neurosci 2014; 17: 923-933.

[32] Vanden Bempt M, Mentens N, Vandenberghe P, Cools J and De Keersmaecker K. EML1-ABL1 is activated by coiled-coil-mediated oligomerization and induces T-cell acute lymphoblastic leukemia or myeloproliferative disease in a mouse bone marrow transplant model. Hemasphere 2018; 2: e32.

[33] Boulard M, Bouvet P, Kundu TK and Dimitrov S. Histone variant nucleosomes: structure, function and implication in disease. Subcell Biochem 2007; 41: 71-89.

[34] Kapoor A, Goldberg MS, Cumberland LK, Ratnakumar K, Segura MF, Emanuel PO, Menendez S, Vardabasso C, Leroy G, Vidal CI, Polsky D, Osman I, Garcia BA, Hernando E and Bernstein E. The histone variant macroH2A suppresses melanoma progression through regulation of CDK8. Nature 2010; 468: 1105-1109.

[35] Konstantinov NK, Ulff-Moller CJ and Dimitrov S. Histone variants and melanoma: facts and hypotheses. Pigment Cell Melanoma Res 2016; 29: 426-433.

Supplementary Methods

Methods

SNP genotyping

In the discovery MDACC CM GWAS dataset, genomic DNA was extracted from CM patients for genotyping using the Illumina HumanOmni-Quad_v1_0_B array. The genotyping data are available from the National Center for Biotechnology Information Database of Genotypes and Phenotypes (dbGaP Study Accession: phs000187.v1.p1). Genome-wide imputation was performed based on the 1000 Genomes Project, phase I v2 CEU, utilizing the MACH software (March 2010 release). Following strict criteria (imputation info score ≥0.8, a genotyping rate ≥95%, a minor allelic frequency ≥5%, and Hardy-Weinberg equilibrium $\geq 1\times10^{-5}$), we extracted SNPs within ± 2 kilobase flanking regions of myeloid cell-related pathway genes from the MDACC CM GWAS dataset. For the NHS/HPFS replication datasets, genotyping of DNA samples was performed with the HumanHap610 array, the Affymetrix 6.0 array, and the Illumina HumanHap550 array. Further imputation was performed depending on haplotype information and genotyped SNPs from 1000 Genomes Project phase II CEU data by applying the MACH program (March 2012 release). The genotyping data were extracted from the NHS/HPFS CM GWAS datasets, following the same quality-control criteria for those from the MDACC CM GWAS dataset.

Statistical methods

For the present study, CMSS was defined as the period from the date of diagnosis of CM to the date of death from CM or the end of follow-up, whichever came first. CM patients known to be alive were censored at the time of the last contact. In the discovery MDACC dataset, we first assessed the associations between all available SNPs in 280 myeloid cell-related pathway genes and CMSS in a single-locus analysis using the GenABEL package of R software. Then multivariable Cox proportional hazards regression analyses were performed with adjustment for available covariates in the MDACC dataset (including age, sex, Breslow thickness, ulceration, distant/regional metastasis, and mitotic rate); however, in the replication NHS/HPFS dataset, the only variables covariates for adjustment were age and sex. In view of the high level of linkage disequilibrium among acquired SNPs, we employed Bayesian false discovery probability (BFDP) with a cutoff value of 0.80 for multiple testing correction to lower the probability of potentially false positive results. In addition, we assigned a prior probability of 0.10 and an upper boundary hazards ratio (HR) of 3.0 for an association with variant genotypes or minor alleles of the SNPs with $P<0.05$. Next, we applyed a multivariable stepwise Cox regression model to identify independent tag SNPs in the MDACC dataset that had more covariate information. We then adopted a meta-analysis to combine the results of the identified SNPs from the MDACC dataset and the NHS/HPFS dataset using PLINK 1.90 with the Cochran's Q statistics and I^2 for heterogeneity test. Because there was no significant heterogeneity between the MDACC dataset and the NHS/HPFS dataset (Q test $P > 0.1$, $I^2 < 25.0\%$), we performed the meta-analysis with a fixed-effects model. We subsequently evaluated the cumulative effects of all identified SNPs by adding up the risk alleles. For the stratified analyses by subgroups, we calculated inter-study heterogeneity and evaluated the interaction. To evaluate the correlation between the identified SNPs and their genes' mRNA expression, we employed expression quantitative trait loci analyses with a linear regression model using data from the 373 European descendants included in the 1,000 Genomes Project, the genotype-tissue expression project, and The Cancer Genome Atlas database using R software (version 3.5.0). Finally, we explored the association between the mRNA expression levels of the genes where the SNPs are located and CM survival using the KM analysis from an online database. All statistical analyses were performed with SAS software (version 9.4; SAS Institute, Cary, NC) unless specified otherwise.

Supplementary Table 1. List of 280 selected genes in the myeloid cell-related pathway

Dataset	Name of pathway	Number of genes
GO	GO_NEGATIVE_REGULATION_OF_MYELOID_CELL_DIFFERENTIATION	92
GO	GO_HEMATOPOIETIC_STEM_CELL_PROLIFERATION	23
GO	GO_HEMATOPOIETIC_PROGENITOR_CELL_DIFFERENTIATION	162
GO	GO_GRANULOCYTE_DIFFERENTIATION	33
REACTOME	REACTOME_RUNX1_REGULATES_TRANSCRIPTION_OF_GENES_INVOLVED_IN_DIFFERENTIATION_OF_MYELOID_CELLS_7	7
KEGG	-	0
BIOCARTA	-	0
PID	-	0
Total	*C1QC, HAX1, LBR, TAL1, ACP6, HES5, KCNAB2, MIXL1, PRRC2C, PSMA5, PSMB2, PSMB4, PSMD4, PTPRC, SSBP3, TP73, WDR78, YTHDF2, CD34, WNT2B, APCS, CDC73, HIST2H4A, HIST2H4B, ITPKB, PIAS3, RBM15, INPP5D, SP3, EIF2AK2, NFE2L2, PLEK, PSMD1, PSMD14, PSME4, SOS1, XRCC5, GPR55, INHA, MEIS1, TMEM178A, ADIPOQ, GATA2, HCLS1, JAGN1, DHX36, HES1, HYAL2, MLF1, PSMD2, PSMD6, TREX1, ARIH2, MECOM, THPO, WNT5A, CLDN18, CTNNB1, GPR171, LTF, TCTA, LEF1, HERC6, KIT, PDGFRA, RBM47, REST, SFRP2, FBXW7, PF4, TLR3, CSF2* *IL5, CSF1R, FNIP1, FST, PDGFRB, TENT2, CARTPT, HSPA9* *IL4, PIK3R1, L3MBTL3, BVES, DACT2, FOXC1, MYB, PDCD2, PSMB1, PSMB8, PSMB9, SOX4, SRF, ZBTB24, DLL1, HIST1H4A, HIST1H4B, HIST1H4C, HIST1H4D, HIST1H4E, HIST1H4F, HIST1H4H, HIST1H4I, HIST1H4J, HIST1H4K, HIST1H4L, RUNX2, ANLN, BRAF, CDK6, INHBA, PSMA2, PSMC2, PTPRZ1, PUS7, SHH, HOXA5, HOXA7, HOXA9, LRRC17, NCAPG2, TRIB1, AGPAT5, CEBPD, ESCO2, PRKDC, RRS1, SFRP1, ZFAT, LYN, MYC* *PTK2B, ABL1, NOTCH1, PSMB7, TLR4, DHTKD1, GATA3, LDB1, MMP21, SPI1, DPF2, JAM3, KMT2A, LMO1, LMO2, PSMA1, PSMC3, PSMD13, YAP1, CTR9, MIR125B1, UBASH3B, ZBTB16, TESC, C12orf29, KRT75, PSMD9, PTPN6, ETV6, KITLG, SART3* *WNT1, WNT10B, HIST4H4, CUL4A, ARHGEF7, ARL11, FLT3, LIG4, N4BP2L2, CEBPE, IL25, BATF, BMP4, EML1, METTL3, PLD4, PSEN1, PSMA3, PSMA6, PSMB11, PSMB5, PSMC1, PSMC6, PSME1, PSME2, SLC8A3, STON2, ZBTB1, GPR68, NFKBIA, ZFP36L1, LGALS3, PSMA4, PYGO1, SIN3A, TCF12, CIB1, FBN1, KLF13, LEO1, MEIS2, WDR61, CBFA2T3, ZFPM1, CBFB, CIAO3, NUDT21, PSMB10, PSMD7, SETD1A, SLC7A6OS, SMPD3, ATXN1L, CREBBP, PRKCB, CSF3, DHRS7B, EVI2B, FASN, RARA, ACE, FLCN, HEATR9, HOXB3, HOXB4, MEOX1, PSMB3, PSMB6, PSMC5, PSMD11, PSMD12, PSMD3, PSME3, TNFRSF13B, TOP2A, CTC1, CCL3, HOXB8, NF1, NME1, NME2, STAT5B, BCL2, PSMA8, SERPINB12, WDR7, PTPN2, CEACAM1, CEBPA, ARMC6, EEF2, ERCC2, FSTL3, PSMC4, PSMD8, SIPA1L3, TCF3, TGFB1, TMEM190, TMEM91, ZNF784, BABAM1, LILRB1, LILRB3, LILRB4, PAF1, PRMT1, ZFP36, ZNF675, ZBTB46, ITCH, PSMA7, PSMF1, MAFB, RUNX1, GABPA, MIR125B2, TOB2* (after removing the duplicated 31 genes, 5 genes in X chromosome, 1 pseudogenes)	280

Keyword: myeloid cell; Organism: Homo sapiens; Website: http://software.broadinstitute.org/gsea/msigdb/search.jsp.

Supplementary Table 2. Distributions of the characteristics of CM patients in the MDACC and Harvard genotyping datasets

Parameter		Frequency		MFT	HR (95% CI)[a]	*P*[a]
		Patient	Death (%)			
MDACC		858	95 (11.1)	81.1		
Age (years)	≤50	371	31 (8.4)	85.8	1.00	
	>50	487	64 (13.1)	78.1	1.69 (1.10-2.59)	0.017
Sex	Female	362	26 (7.2)	85.9	1.00	
	Male	496	69 (13.9)	77.8	2.07 (1.32-3.25)	0.002
Regional/distant metastasis	No	709	51 (7.2)	82.7	1.00	
	Yes	149	44 (29.5)	69.4	4.78 (3.19-7.15)	<0.001
Breslow thickness (mm)	≤1	347	7 (2.0)	85.0	1.00	
	>1	511	88 (17.2)	78.1	9.17 (4.25-19.80)	<0.001
Ulceration	No	681	48 (7.1)	84.0	1.00	
	Yes	155	43 (27.7)	64.3	4.91 (3.29-7.42)	<0.001
	Missing	22				
Mitotic rate (mm^2)	≤1	275	9 (3.3)	82.2	1.00	
	>1	583	86 (14.8)	80.1	4.67 (2.35-9.29)	<0.001
Harvard		409	48 (11.5)	179.0		
Age (years)	≤50	72	3 (4.2)	352.5	1.00	
	>50	337	45 (13.4)	167.0	4.04 (1.25-13.06)	0.020
Sex	Female	271	31 (11.4)	198.0	1.00	
	Male	138	17 (12.3)	155.5	1.16 (0.64-2.10)	0.622

Abbreviations: CM, cutaneous melanoma; MDACC, The University of Texas MD Anderson Cancer Center; MFT, median follow-up time (months); HR, hazards ratio; CI, confidence interval. [a]Univariate Cox proportional hazards regression analysis.

Supplementary Table 3. Functional prediction of 22 validated SNPs in high linkage disequilibrium (LD) ($r^2 \geq 0.8$) in myeloid cell-related pathway genes

SNP	Chr	Position (hg38)	Gene	Haploreg v4.12[1]							
				LD (r^2)	Promoter histone marks	Enhancer histone marks	DNAse	Proteins bound	Motifs changed	GRASP QTL hits	Selected eQTL hits
rs1175649	1	112476655	*WNT2B*	1		ESC			4 altered motifs		6 hits
rs1175650	1	112476952	*WNT2B*	1					GR, ZID		8 hits
rs2798245	1	112464917	*WNT2B*	1		15 tissues	6 tissues		5 altered motifs		7 hits
rs11751812	6	26187334	*HIST1H4D*	1	ESC, IPSC	5 tissues			Smad3	12 hits	18 hits
rs11754140	6	26186976	*HIST1H4D*	1		4 tissues			10 altered motifs		10 hits
rs6906367	6	26187125	*HIST1H4D*	1	ESC	4 tissues	ESDR		5 altered motifs	13 hits	14 hits
rs11757394	6	26206694	*HIST1H4E*	1	22 tissues	5 tissues	26 tissues	5 bound proteins	DMRT4, Irf, LBP-9		8 hits
rs2069018	6	26205718	*HIST1H4E*	0.97	23 tissues		49 tissues	22 bound proteins	4 altered motifs	7 hits	14 hits
rs2069019	6	26205604	*HIST1H4E*	1	23 tissues		53 tissues	25 bound proteins	Nanog		8 hits
rs2069020	6	26205500	*HIST1H4E*	1	23 tissues		49 tissues	18 bound proteins	5 altered motifs		8 hits
rs56186759	6	26207181	*HIST1H4E*	1	14 tissues	12 tissues	MUS, OVRY	POL2, POL24H8	COMP1		8 hits
rs56220351	6	26206884	*HIST1H4E*	1	16 tissues	12 tissues			4 altered motifs		8 hits
rs16891407	6	26206299	*HIST1H4E*	1	23 tissues		53 tissues	15 bound proteins	STAT	7 hits	18 hits
rs77205516	6	26205128	HIST1H4E	1	23 tissues		27 tissues	4 bound proteins	Zfp105		8 hits
rs16891481	6	26242777	*HIST1H4F*	1	GI	5 tissues			Barhl1, Hoxa5	12 hits	17 hits
rs3734533	6	26240624	*HIST1H4F*	0.96	21 tissues	BRST	46 tissues	16 bound proteins	4 altered motifs	22 hits	15 hits
rs41521949	11	122597367	*UBASH3B*	1	BLD	11 tissues	6 tissues		4 altered motifs		1 hits
rs73018235	11	122599673	*UBASH3B*	1	BLD	9 tissues	KID, THYM		GR, LXR, STAT		1 hits
rs73018236	11	122600620	*UBASH3B*	1		BLD, HYM, SPLN			Pax-5, Zbtb3, Znf143		1 hits
rs7952454	11	122597548	*UBASH3B*	1	4 tissues	16 tissues	5 tissues		7 altered motifs		1 hits
rs61959910	13	50207885	*ARL11*	1		BLD, HRT, VAS		GATA2	4 altered motifs		
rs10151787	14	100266973	*EML1*	1					Crx, Pax-4		

Abbreviations: SNP, single-nucleotide polymorphism; Chr, chromosome; DNAse, deoxyribonuclease; QTL, quantitative trait loci; eQTL, expression quantitative trait loci; [1]Haploreg: https://pubs.broadinstitute.org/mammals/haploreg/haploreg.php.

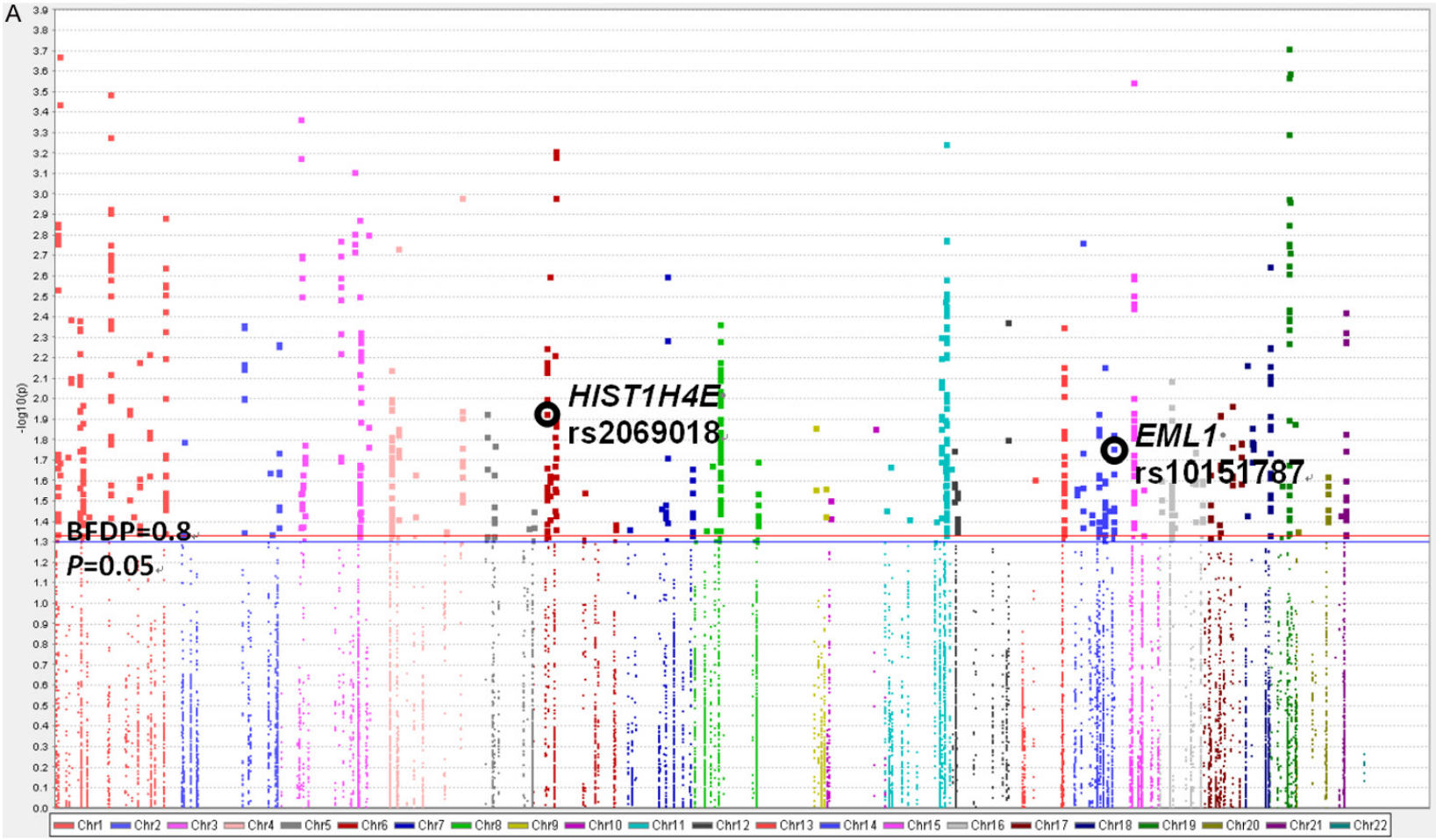
A
-log10(p)
HIST1H4E
rs2069018
EML1
rs10151787
BFDP=0.8
P=0.05
Chr1 Chr2 Chr3 Chr4 Chr5 Chr6 Chr7 Chr8 Chr9 Chr10 Chr11 Chr12 Chr13 Chr14 Chr15 Chr16 Chr17 Chr18 Chr19 Chr20 Chr21 Chr22

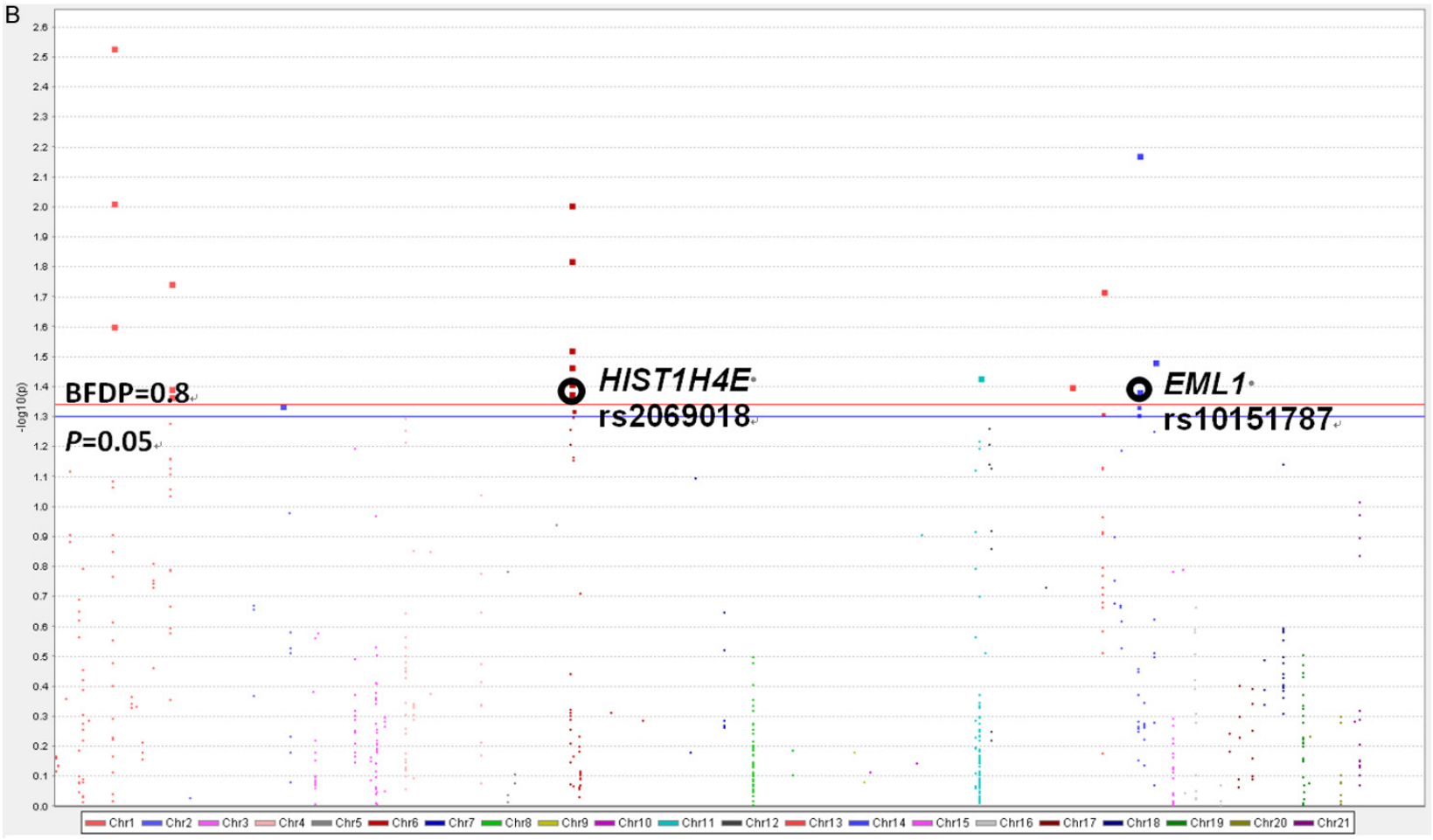

Supplementary Figure 1. Manhattan plot. A. Manhattan plot for 24,855 SNPs in the MDACC study. B. Manhattan plot for 1126 SNPs in the NHS/HPFS study. The blue horizontal line indicates *P* value equal to 0.05 and the red horizontal line represents BFDP value equal to 0.8. Abbreviations: SNP, single-nucleotide polymorphism; MDACC, The University of Texas MD Anderson Cancer Center; NHS/HPFS, Nurses' Health Study/Health Professionals Follow-up Study; BFDP, Bayesian false-discovery probability.

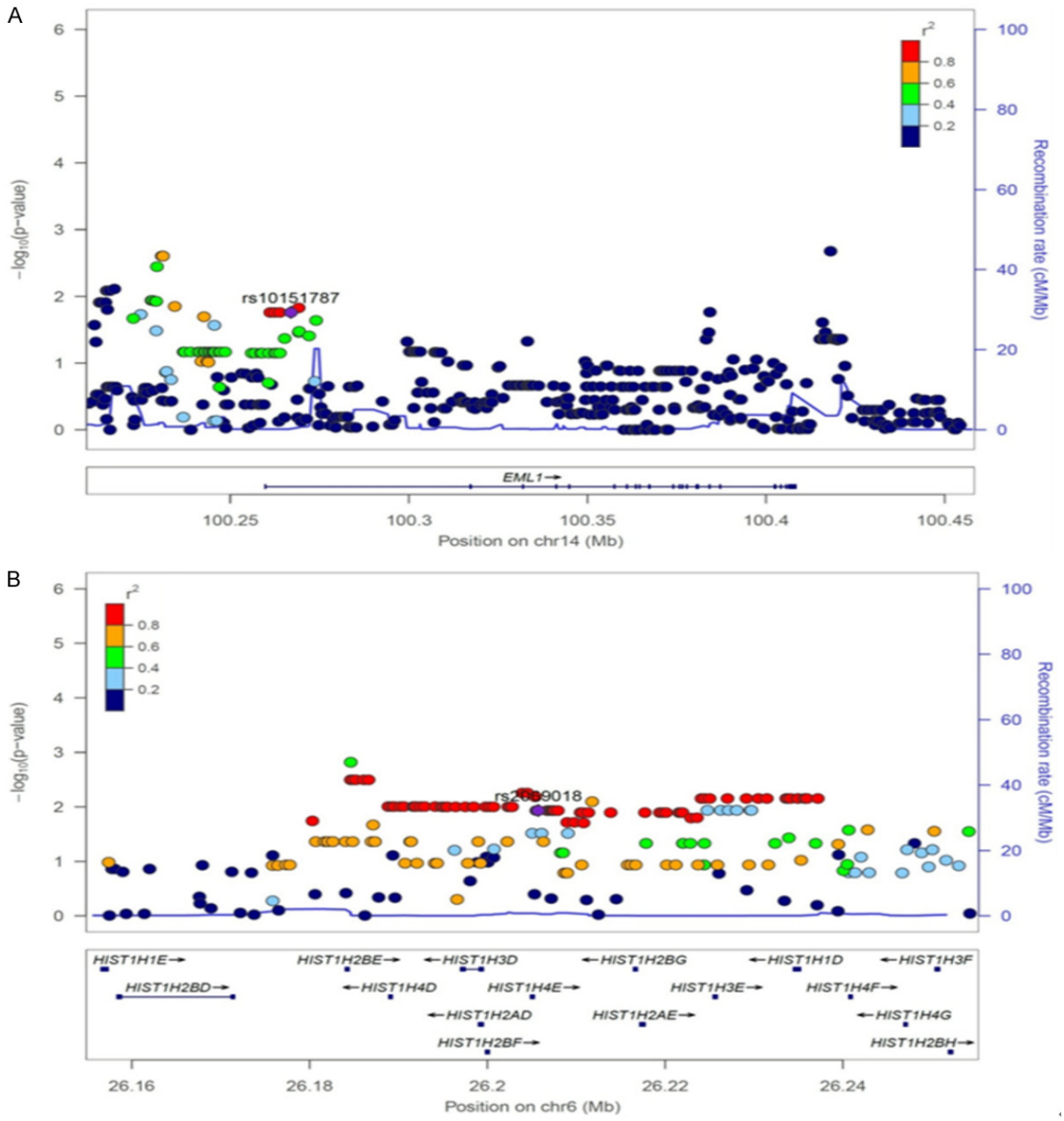

Supplementary Figure 2. Regional association plots for *EML1* rs10151787 and *HIST1H4E* rs2069018. Regional association plots contained 50 kb up and downstream of the gene regions in *EML1* (A) and *HIST1H4E* (B).

Supplementary Table 4. Stratified Cox analysis for risk alleles of the significant SNPs identified in the MDACC and NHS/HPFS genotyping datasets

Characteristics	0-1 risk allele[a]		2-4 risk alleles[a]		Univariate analysis		Multivariate analysis[b]		Interaction[c]
	All	Death (%)	All	Death (%)	HR (95% CI)	*P*	HR (95% CI)	*P*	
MDACC									
Age (years)									
≤ 50	321	22 (6.85)	50	9 (18.00)	2.68 (1.23-5.83)	0.013	2.62 (1.18-5.86)	0.019	
> 50	415	47 (11.33)	72	17 (23.61)	2.37 (1.36-4.13)	0.002	2.63 (1.47-4.72)	0.001	0.730
Sex									
Male	424	51 (12.03)	72	18 (25.00)	2.33 (1.36-3.99)	0.002	2.29 (1.32-4.00)	0.003	
Female	312	18 (5.77)	50	8 (16.00)	2.89 (1.26-6.66)	0.013	2.95 (1.24-7.00)	0.014	0.507
Stage									
I/II	615	35 (5.69)	94	16 (17.02)	3.22 (1.78-5.83)	<0.001	4.37 (2.36-8.08)	<.0001	
III/IV	121	34 (28.10)	28	10 (35.71)	1.41 (0.70-2.85)	0.343	1.27 (0.59-2.74)	0.537	0.297
Breslow thickness (mm)									
≤1	306	5 (1.63)	41	2 (4.88)	3.07 (0.60-15.83)	0.180	2.76 (0.06-9.05)	0.829	
>1	430	64 (14.88)	81	24 (29.63)	2.26 (1.42-3.62)	0.0006	2.54 (1.58-4.09)	0.0001	0.956
Ulceration									
No	585	36 (6.15)	96	12 (12.50)	2.10 (1.09-4.05)	0.026	1.91 (0.98-3.74)	0.058	
Yes	131	30 (22.90)	24	13 (54.17)	3.34 (1.74-6.42)	<0.001	3.23 (1.67-6.25)	0.0005	0.573
Missing	22								
Mitotic rate (mm^2)									
≤1	230	6 (2.61)	45	3 (6.67)	2.65 (0.66-10.61)	0.168	3.34 (0.56-19.43)	0.179	
>1	506	63 (12.45)	77	23 (29.87)	2.72 (1.69-4.39)	<.0001	2.50 (1.53-4.10)	0.0003	0.467
NHS/HPFS									
Age (years)									
≤ 50	61	2 (3.28)	11	1 (9.09)	2.78 (0.25-30.69)	0.403	2.87 (0.26-31.70)	0.391	
> 50	299	37 (12.37)	38	8 (21.05)	1.74 (0.81-3.73)	0.156	1.74 (0.81-3.73)	0.157	0.757
Sex									
Male	124	14 (11.29)	14	3 (21.43)	1.71 (0.49-5.96)	0.401	2.05 (0.57-7.41)	0.276	
Female	236	25 (10.59)	35	6 (17.14)	1.70 (0.70-4.13)	0.246	1.85 (0.76-4.52)	0.178	0.816

Abbreviations: SNP, single-nucleotide polymorphism; MDACC, The University of Texas MD Anderson Cancer Center; NHS, the Nurses' Health Study; HPFS, the Health Professionals Follow-up Study; HR, hazards ratio; CI, confidence interval. [a]Risk alleles include *EML1* rs10151787 G allele and *HIST1H4E* rs2069018 C allele; [b]Adjusted for age, sex, Breslow thickness, stage, ulceration and mitotic rate in Cox models of SNPs and CMSS in the MDACC dataset and adjusted for age and sex only in the NHS/HPFS datasets; [c]Interaction: the interaction between the risk alleles and each clinical variable.

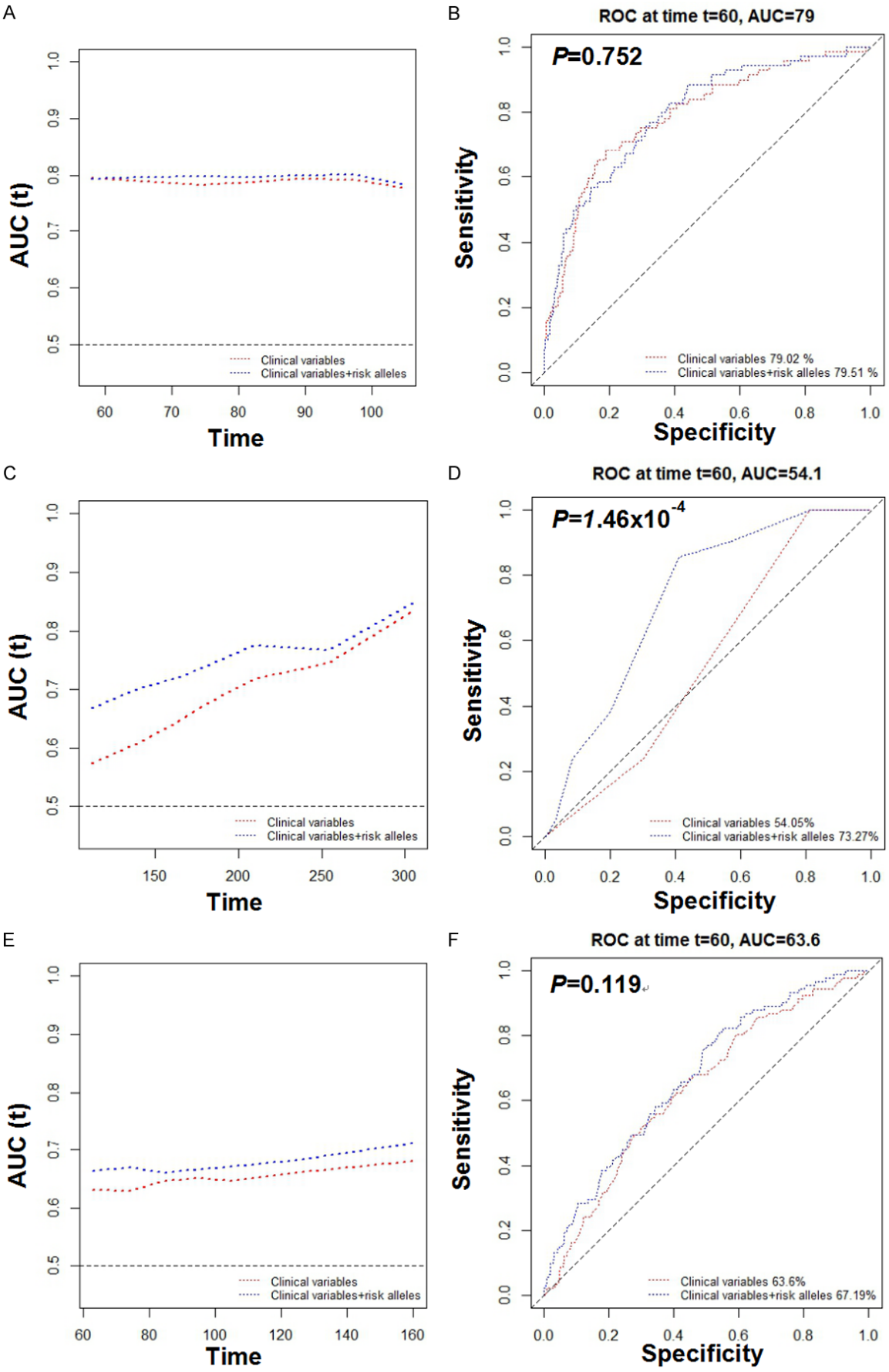
A
AUC (t)
Time
Clinical variables
Clinical variables+risk alleles
B
ROC at time t=60, AUC=79
P=0.752
Sensitivity
Specificity
Clinical variables 79.02 %
Clinical variables+risk alleles 79.51 %
C
AUC (t)
Time
Clinical variables
Clinical variables+risk alleles
D
ROC at time t=60, AUC=54.1
P=1.46x10-4
Sensitivity
Specificity
Clinical variables 54.05%
Clinical variables+risk alleles 73.27%
E
AUC (t)
Time
Clinical variables
Clinical variables+risk alleles
F
ROC at time t=60, AUC=63.6
P=0.119
Sensitivity
Specificity
Clinical variables 63.6%
Clinical variables+risk alleles 67.19%

Supplementary Figure 3. ROC curve and time-dependent AUC estimation for five-year CMSS prediction in CM patients. The Time-dependent AUC estimation based on clinical variables plus risk alleles in the MDACC dataset (A), the NHS/HPFS dataset (C) and the combined MDACC and NHS/HPFS dataset (E). The five-year CMSS prediction by ROC curve in the MDACC dataset (B), the NHS/HPFS dataset (D) and the combined MDACC and NHS/HPFS dataset (F). Abbreviations: CMSS, cutaneous melanoma-specific survival; SNP, single-nucleotide polymorphism; AUC, area under receiver curve; MDACC, The University of Texas MD Anderson Cancer Center; NHS/HPFS, Nurses'Health Study/Health Professionals Follow-up Study; ROC, receiver operating characteristic.

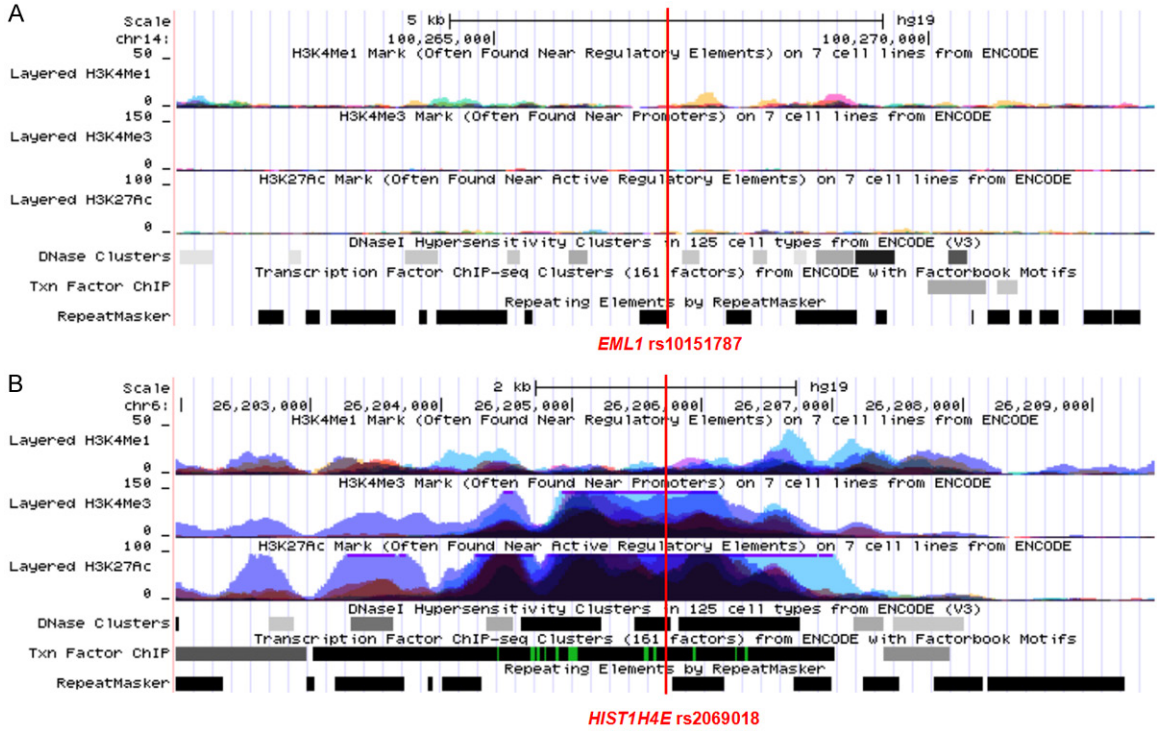

Supplementary Figure 4. Functional prediction of EML rs10151787 and HIST1H4E rs2069018 in the ENCODE data. Location and functional prediction of *EML* rs10151787 (A). Location and functional prediction of *HIST1H4E* rs2069018 (B). The H3K27Ac, H3K4Me1, and H3K4Me3 tracks showed the genome-wide levels of enrichment of acetylation of lysine 27, the mono-methylation of lysine 4, and tri-methylation of lysine 4 of the H3 histone protein. DNase clusters track showed DNase hypersensitivity areas. Tnx factor track showed regions of transcription factor binding of DNA.

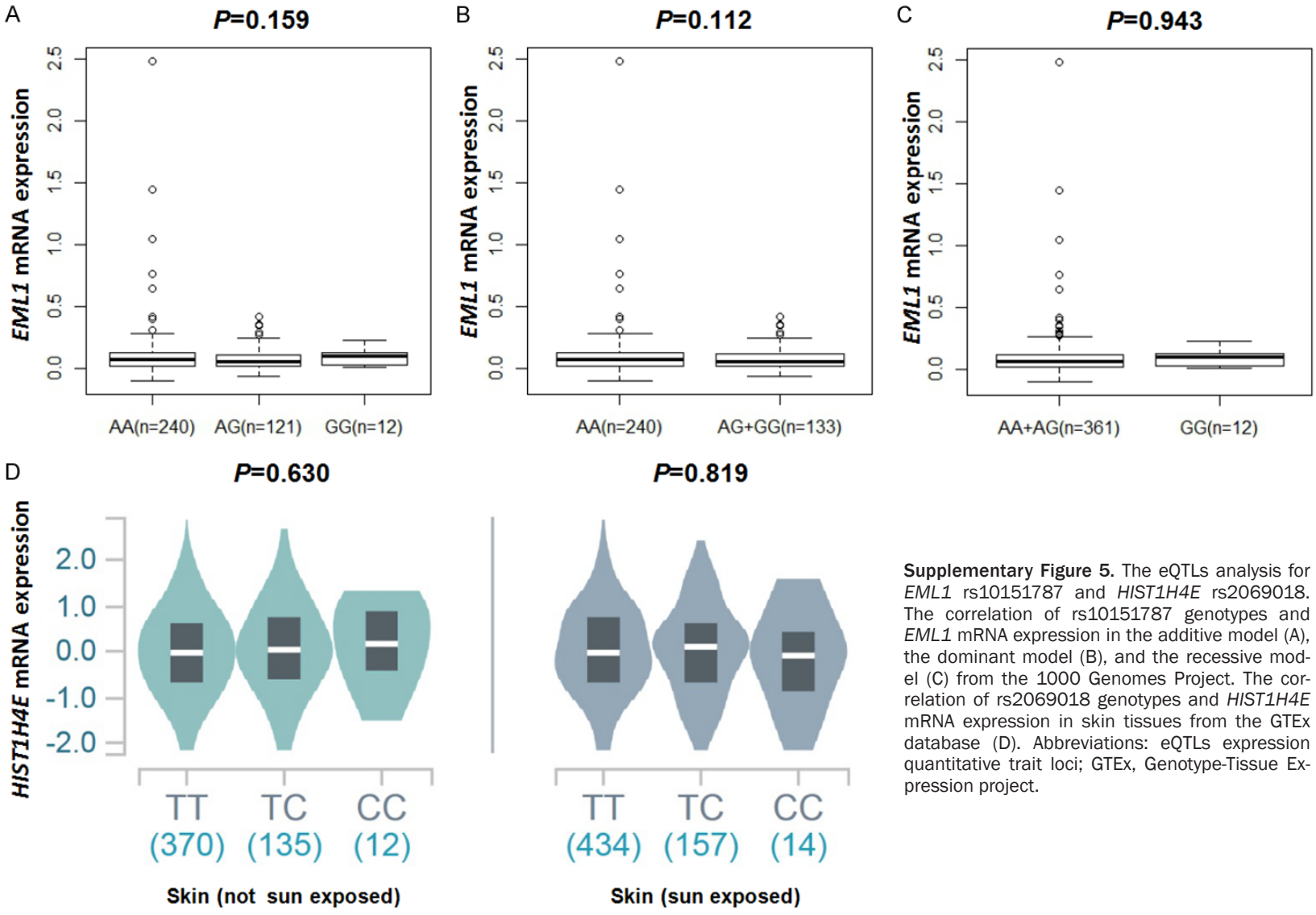

Supplementary Figure 5. The eQTLs analysis for *EML1* rs10151787 and *HIST1H4E* rs2069018. The correlation of rs10151787 genotypes and *EML1* mRNA expression in the additive model (A), the dominant model (B), and the recessive model (C) from the 1000 Genomes Project. The correlation of rs2069018 genotypes and *HIST1H4E* mRNA expression in skin tissues from the GTEx database (D). Abbreviations: eQTLs expression quantitative trait loci; GTEx, Genotype-Tissue Expression project.

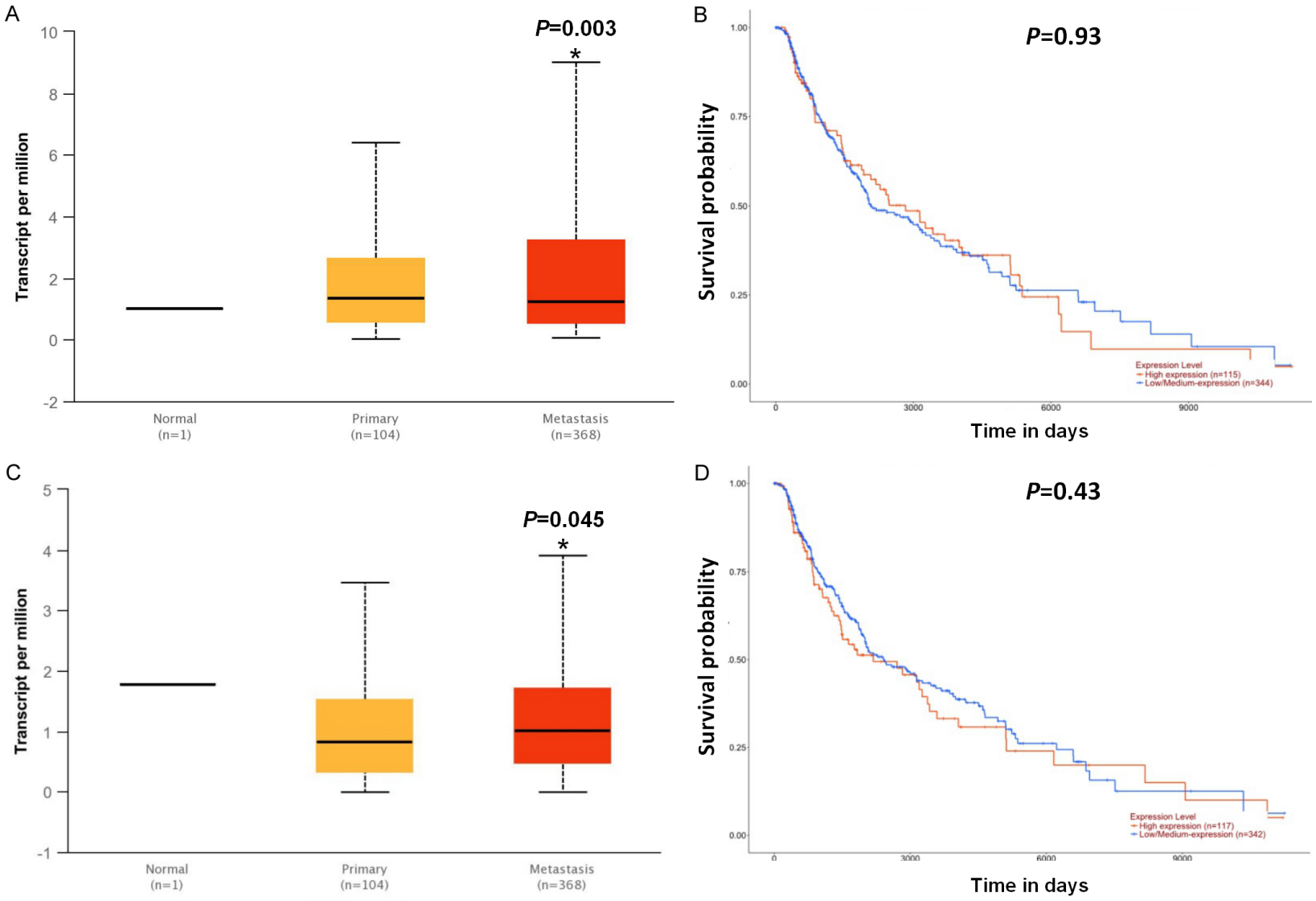

Supplementary Figure 6. Differential mRNA expression analysis and survival prediction in the TCGA database. The difference of *EML1* (A) and *HIST1H4E* (C) mRNA expression between primary melanoma tissues and metastatic melanoma tissues in the TCGA database; *EML1* mRNA expression showed no significant correlation with melanoma survival probability in the TCGA database (B). *HIST1H4E* mRNA expression showed no significant correlation with melanoma survival probability in the TCGA database (D). Abbreviation: TCGA, The Cancer Genome Atlas.